CanVeg

March 18, 2024

This document provides background and literature supporting the Matlab version of Canveg.

This version was developed in 2020 and is applied to an alfalfa canopy and tested with eddy flux data. The goal is to use the new version to help interpret results from our NASA ECOSTRESS project.

The current version has been parameterized for alfalfa and tules.

Canveg is a coupled biophysical model that computes water, CO_2, sensible heat and energy fluxes from vegetated canopies. It has also been applied to study stable isotopes (Baldocchi & Bowling, 2003, Oikawa *et al.*, 2017) and isoprene (Baldocchi *et al.*, 1999). It was originally developed in C and applied to a deciduous forest (Baldocchi & Harley, 1995, Baldocchi & Wilson, 2001, Baldocchi *et al.*, 2002). Over the years I have tried to simplify and generalize the model for a variety of vegetation types (Baldocchi & Meyers, 1998).

The intent of the model is to digest a simple set of meteorological variables above a plant canopy and use that information that drives algorithms that can compute the microclimate within the vegetation and the fluxes of mass and energy between vegetation, the soil and the atmosphere.

The model is multi-layered one dimensional. This version is coded in Matlab and the model was re-casted in matrix form for faster execution. The model operates with n columns for each layer in the canopy and atmosphere and m rows for each half-hourly input. The model is mostly diagnostic and many subroutines are analytical equations for leaf temperature, evaporation, and photosynthesis (Baldocchi, 1994); details of the equations used are reported in the appendix of the cited paper (Baldocchi *et al.*, 1999). A schematic of the model is shown in Figure 1.

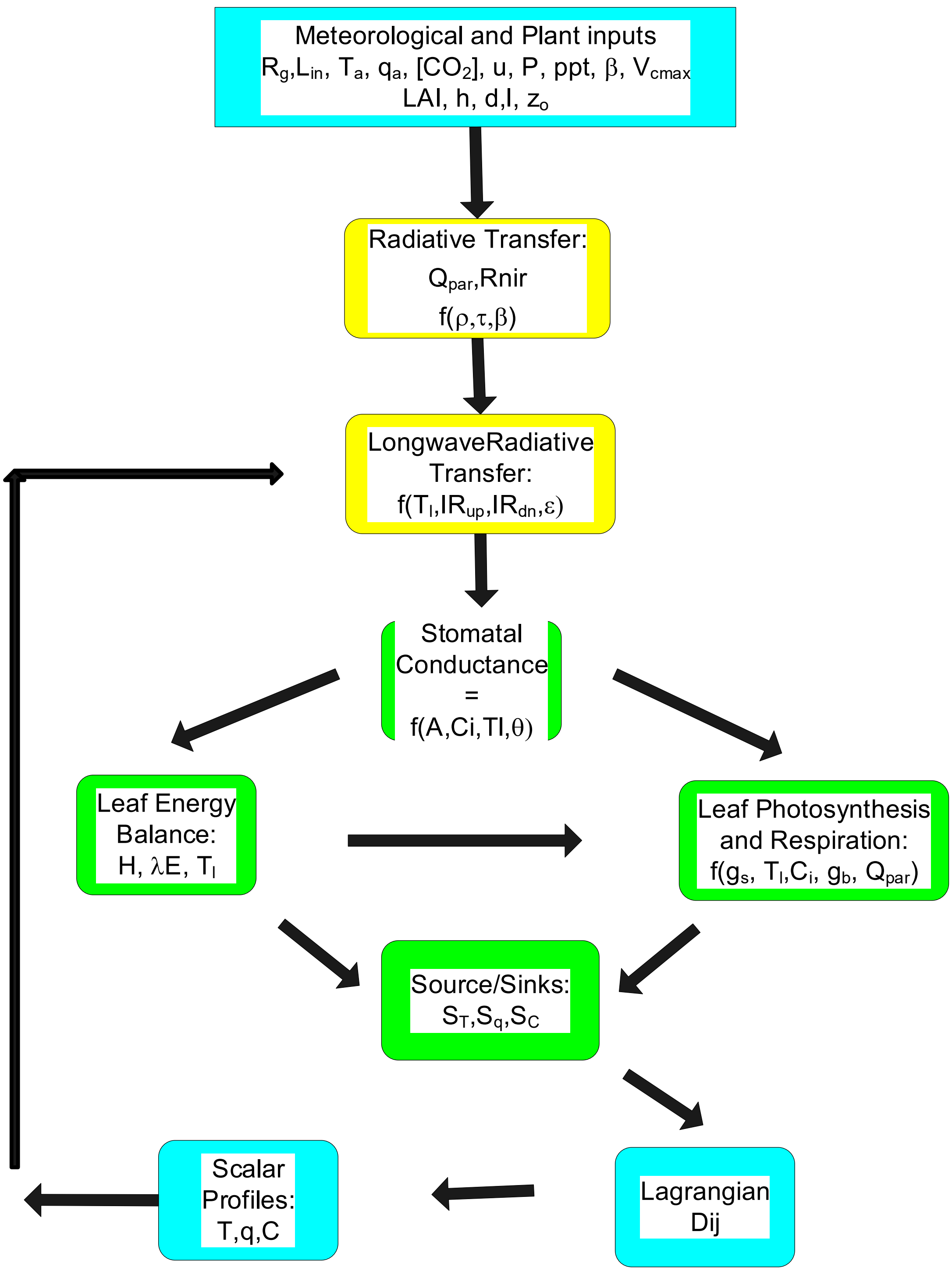

Figure 1 Schematic of the CanVeg model

Conceptually, the model first computes radiative transfer of shortwave visible and near infrared radiation into and out of the vegetation (Norman, 1979). These energy fluxes drive an energy balance model (Paw U & Gao, 1988, Raschke, 1960) that then is used to compute infrared radiation fluxes, latent and sensible heat exchange and leaf temperature. This new information on IR fluxes is used to re-inform energy balance computations, which are repeated in an iterative fashion.

Because many of the functions are non-linear, the model computes fluxes separately on the sunlit and shaded fractions of each layer (Norman, 1981, Norman, 1993).

Leaf energy balance depends upon stomatal conductance. We compute stomatal conductance with a model that is dependent upon photosynthesis, so this requires a photosynthesis module (Collatz *et al.*, 1991). Photosynthesis is computed with the widely used Farquhar, von Caemmerer, Berry model (Farquhar *et al.*, 1980). Once sources and sinks are estimated we compute profiles of scalars, using a Lagrangian random walk model (Raupach, 1987). These new estimates of scalar fields are also used to update and refine computations of sources and sinks.

At present we are running the model through 15 iterations, which seems to make convergence.

The vegetation module overlies soil module that computes heat and moisture transfer (Campbell, 1985).

The architectural flow chart of the code runs as follows.

Subroutines	
`[prm]=parameter_alfalfa();`	Reads all the model parameters as a structure
`[DIJ]=DispCanveg_v2a(prm);`	Compute the Dispersion matrix. It only changes with LAI, so it can be run once, and output can be saved and read for future runs
`inmet=csvread('AlfMetBouldinInput.csv');`	Input meteorological conditions; check code for inputs and their order. Day, hour, solar radiation, air temperature, humidity, wind speed, friction velocity, pressure, CO2 concentration are main inputs. Also can add aerodynamic height, inferred LAI, and water table.
`[soil]=fSetSoilAlfalfa(met,prm);`	Set and input soil parameters
`[quantum,nir,ir,Qin,rnet,Sun,Shade] =fZeroArrays(prm);`	Zero and pre-allocate Arrays for faster execution
`sunang= fSunAngle(prm.time_zone,prm.lat_deg, prm.long_deg, met.day, met.hhour);`	Compute sun angles
`[sunrad]=fDiffuse_Direct_Radiation (met.rglobal,met.parin,met.P_kPa, sunang.sine_beta);`	Computes fraction of direct and diffuse light to apply the model on sun and shaded leaf fractions
`[leafang]=LeafAngle(sunang, prm);`	Computes the G function, the direction cosine between leaf normal and the sun for

	prescribed leaf angle distributions
`[prof]=initial_profile_Matrix(met,prm);`	Pre-allocates arrays for profiles of scalars and fluxes
`[prof.wind]=fUZ_Matrix(met,prm);`	Computes empirical wind speed profile in canopy to estimate boundary layer conductances
`[quantum]=fRadTranCanopy_MatrixV2(sunang,leafang, quantum,waveband,prm);`	Computes Radiative transfer for specific wave bands, eg PAR, NIR. If you have spectral information you look at narrow wave bands, SIF, etc
`[nir]=fRadTranCanopy_MatrixV2(sunang,leafang, nir,waveband,prm);`	Computes Radiative transfer for specific wave bands, eg PAR, NIR. If you have spectral information you look at narrow wave bands, SIF, etc
Start Iteration Loop {…	
`[ir]= fIR_RadTranCanopy_Matrix(leafang,ir, quantum,met,Sun,Shade, prm);`	Computes IR fluxes based on information on leaf temperature
`[Qin]=fQin_Matrix(quantum,nir,ir,prm);`	Computes incoming longwave and shortwave energy absorbed by each layer
`[Sun,Shade]=fEnergy_Carbon_Fluxes_Matrix(Sun, Shade, Qin, quantum, met, prof, prm);`	Computes carbon, water and energy fluxes for each layer for sun and shaded leaf fractions. This master sub routine calls routines for leaf boundary layer resistance, leaf energy balance and photosynthesis. Leaf -air temperature is used to assess whether the boundary layer is affected by convection or free convection.
`[soil]=fSoilEnergyBalanceMatrix(quantum, nir,ir, met, prof, prm, soil,j);`	Compute Soil Energy balance Fluxes
`[prof.Tair_K]=fConcMatrix(prof.H,soilflux, prof.delz, Dij,met,met.T_air_K, prm, fact.heatcoef);`	Compute sources and sink strengths and use them and Dij to compute scalar profiles for air temperature, humidity and CO2.
End Iteration Loop	
	Sum Layers and compute Canopy fluxes weighted for sun/shade fractions

	Plot and visualize

The model is being tested with a set of data from days 141 to 157, 2019 over Bouldin Alfalfa, an Ameriflux site in northern California, between Rio Vista and Lodi (https://ameriflux.lbl.gov/sites/siteinfo/US-Bi1).

For this test, the canopy was fully developed, with a leaf area index of about 6 and a height of 0.85 m. We assume the leaves were 2.5 cm in length and that the leaf angle distribution was spherical.

Parameterizations

We are basing these computations on the fact that alfalfa are amphistomatous. Prior to model developed I rederived the leaf energy balance equations from scratch. These equations are in a separate document

We collected original data for the leaf photosynthesis model using A-Ci measurements from the field

August 31, Camilo has update on parameters

Vcmax=170.9 +- 4.95 umol m-2 s-1 (mean +- std error)
Jmax= 258.6 +- 10.15 umol m-2 s-1 (mean +- std error)

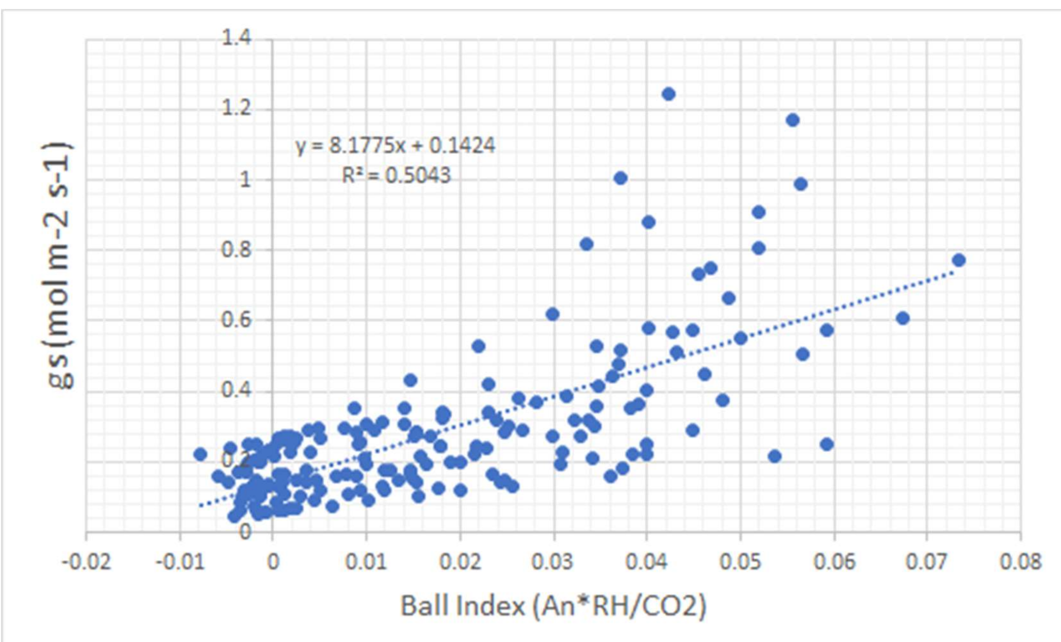

Vcmax and Jmax was computed using the Sharkey algorithms (Sharkey *et al.*, 2007) based on measurements between Sep 2019 to August 2020 (n=25), the averages and the standard error are:

Vcmax= 165 +- 5.54 umol m-2 s-1

Jmax= 260 +- 12.41 umol m-2 s-1
Rd= 2.68 +- 0.09 umol m-2 s-1

The Sharkey function computed these for 25 C.

I needed to adjust the Boltzmann functions to normalize to 25 C. The older code was set to Topt.

There is essentially no published data on alfalfa stomatal conductance in the literature

Ball Berry coefficient were derived from the gas exchange measurements of Dr. Camilo Rey Sanchez. He derived these coefficients from Light Response Curves on alfalfa leaves in the field.

Here is a curve from 2020. Circa Aug 2021 was finding the model was computing LE too too large using the other bb slope of 11.8. Using the smaller, 9 value, is giving very good LE and Ps values

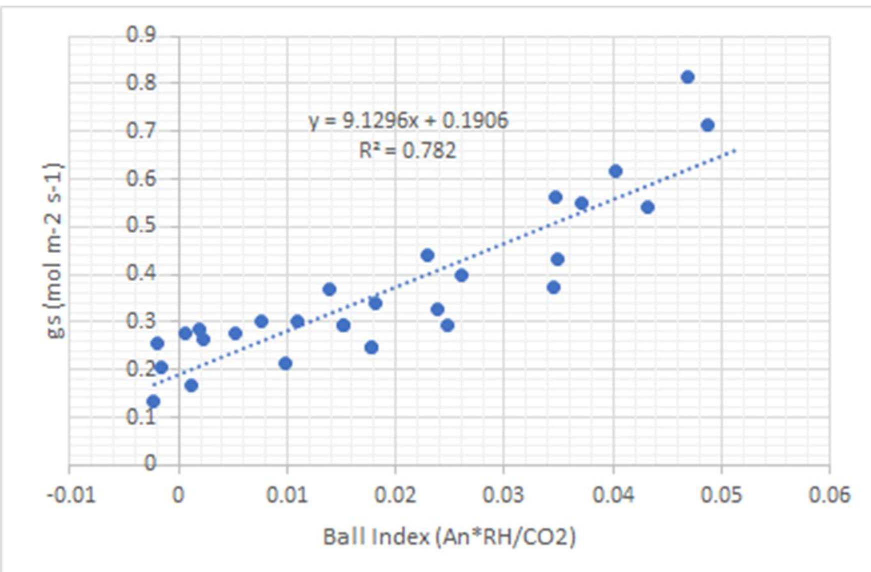

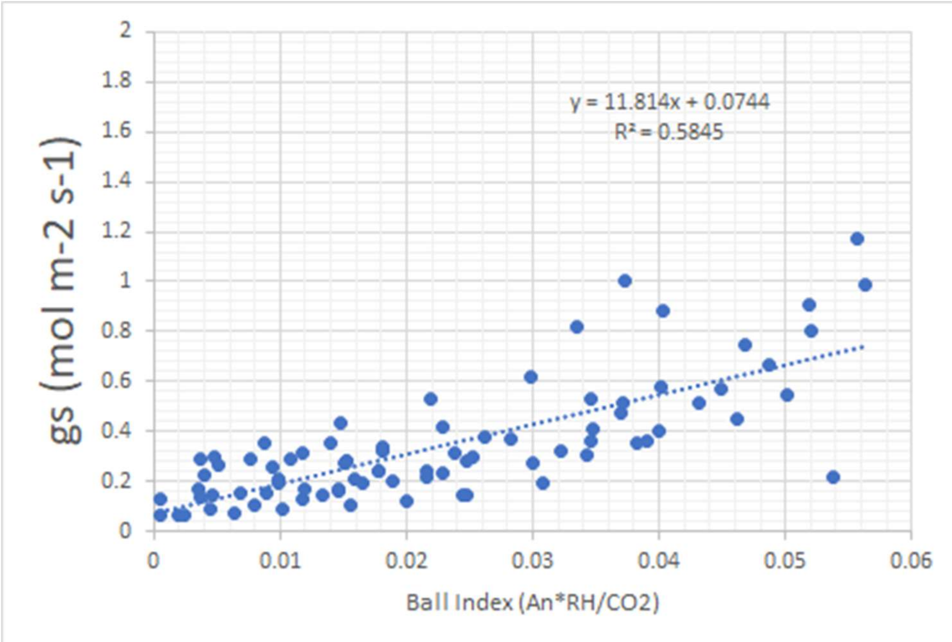

We discovered that the intercept of the Ball Berry model was much larger than most observations in the literature. And, the large values were causing LE to be too big at night and H to be to negative during the day. We downscaled g0 based on data from other studies (Franks *et al.*, 2018, Medlyn *et al.*, 2011, Xu & Baldocchi, 2003).

The next figure shows an estimate of g0 from an A-Ci curve on alfalfa that is much smaller than the previous data. This data set was collected on a very hot day, 35 C and greater, on August, 2019. So, we are reluctant to use these data instead. Plus these data are confined to CO2 concentrations near ambient. The figure is more scattered if the whole A-Ci curve is used.

Alfalfa, Aug 2019, from A-Ci curve

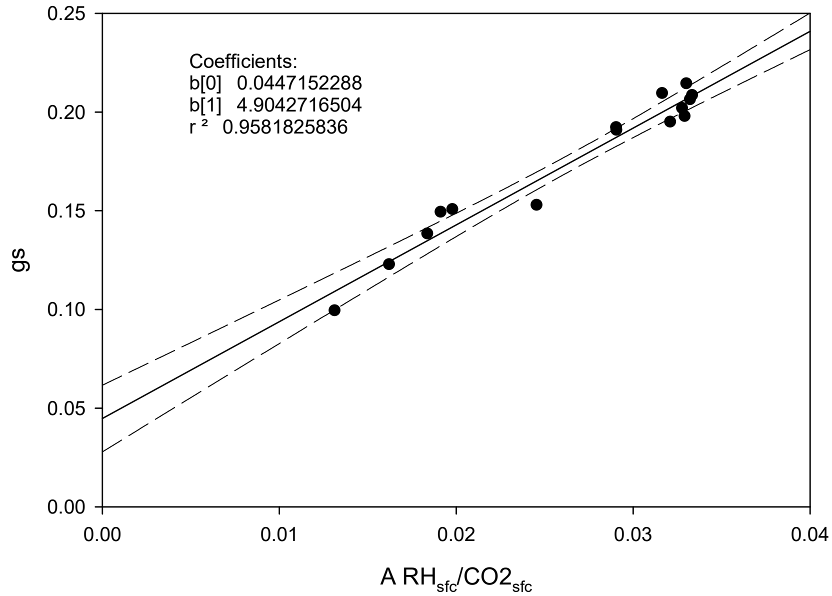

Xu finds a tiny value for g0 for blue oak. When collecting these data, Xu would take 20 minutes for stomata to adjust to get high precision values; the scatter is much smaller compared to the r2 of 0.54 shown above. Our quickly attained values may account for the larger degree of scatter seen above; leaks through seals can play a role, too, explaining the higher than expected value for g0.

Tonzi oak leaf, tree #92, Li-Cor 6400 measurement, 2001

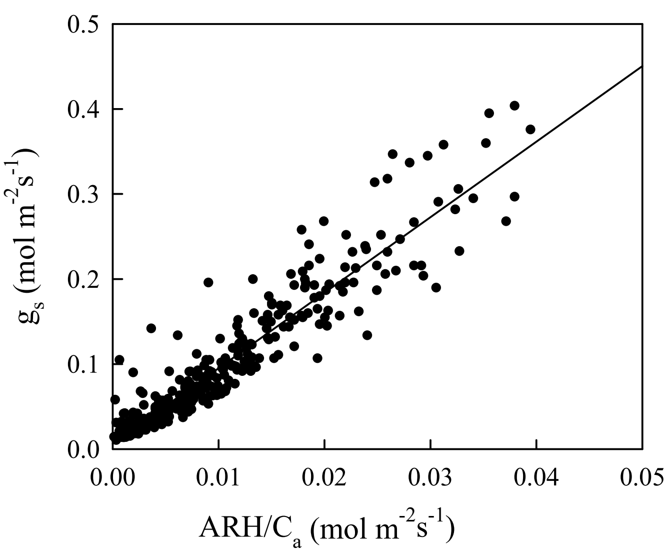

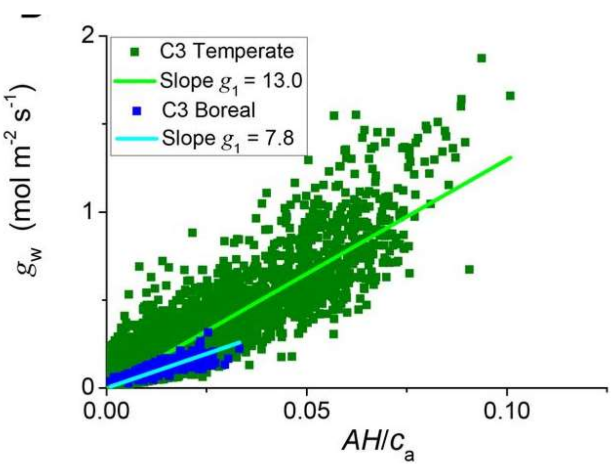

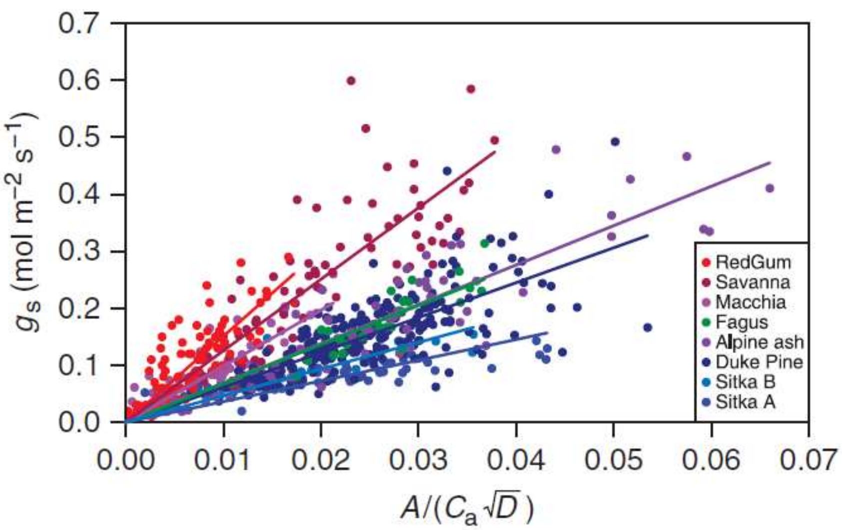

The Licor 6400 was correctly adjusted to consider amphistomatous leaves. We applied the following theory to compute total leaf conductance to water vapor.

Stomatal Conductance to Water Vapor

The stomatal conductance g_{sw} to water vapor (mol H_2O m^{-2} s^{-1}) is obtained from the total conductance by removing the contribution from the boundary layer.

$$g_{sw} = \frac{1}{\frac{1}{g_{tw}} - \frac{k_f}{g_{bw}}} \tag{1-9}$$

where k_f is a factor based on the estimate K of the fraction of stomatal conductances of one side of the leaf to the other (termed *stomatal ratio* throughout this manual),

$$k_f = \frac{K^2 + 1}{(K + 1)^2} \tag{1-10}$$

and g_{bw} is the boundary layer conductance to water vapor (mol H_2O $m^{-2}s^{-1}$) from one side of the leaf. The boundary layer conductance correction thus depends on whether the leaf has stomata on one or both sides of the leaf.

Leaf Reflectance and Transmittance

UCD presentation shows NIR reflectance and transmittance are about the same

June 4, 2019

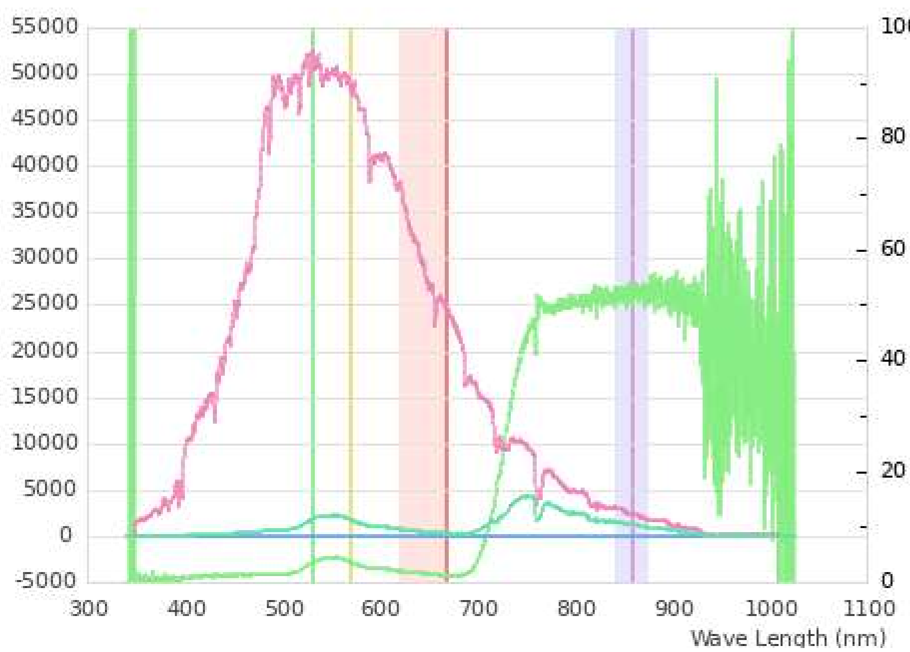

Ocean Optics Sept 17, 2019

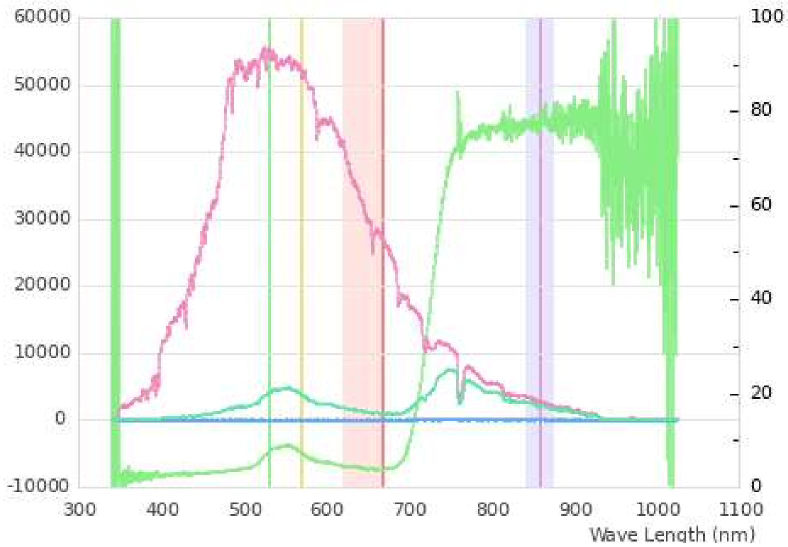

May 2, 2019.. Alfalfa had been cut

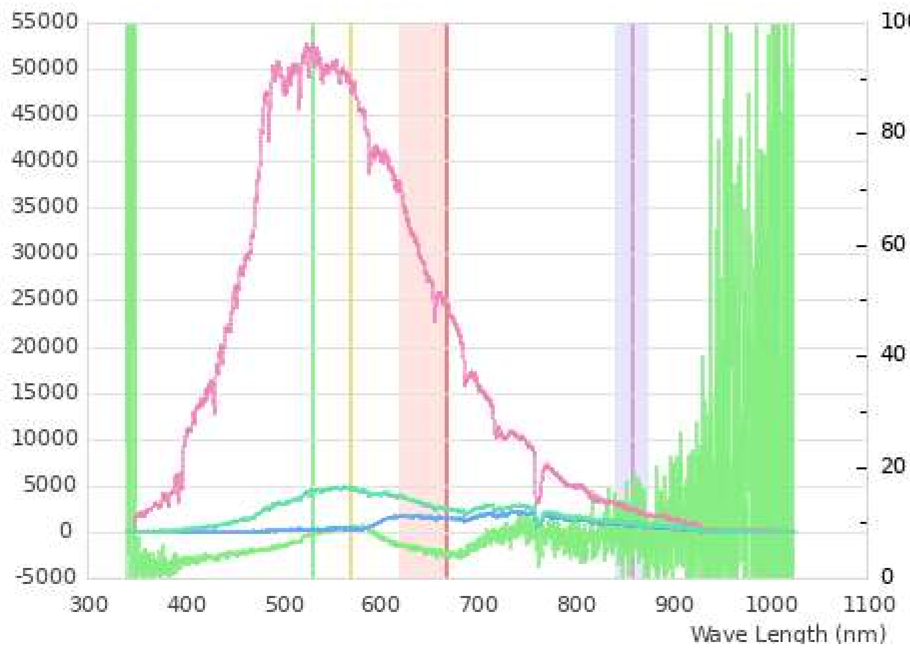

The literature has a couple of papers with leaf spectra in the PAR and NIR bands

van der Tol, Christiaan, Micol Rossini, Sergio Cogliati, Wouter Verhoef, Roberto Colombo, Uwe Rascher, and Gina Mohammed. 2016. 'A model and measurement comparison of diurnal cycles of sun-induced chlorophyll fluorescence of crops', *Remote Sensing of Environment*, 186: 663-77.

Applied SCOPE to alfalfa

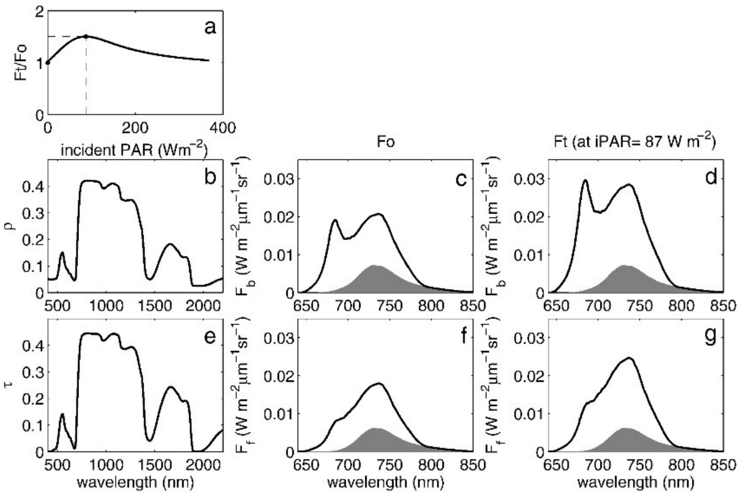

Another paper reports data from LOPEX study in Germany, which may be a similar site as used by van del Tol and the SCOPE team.

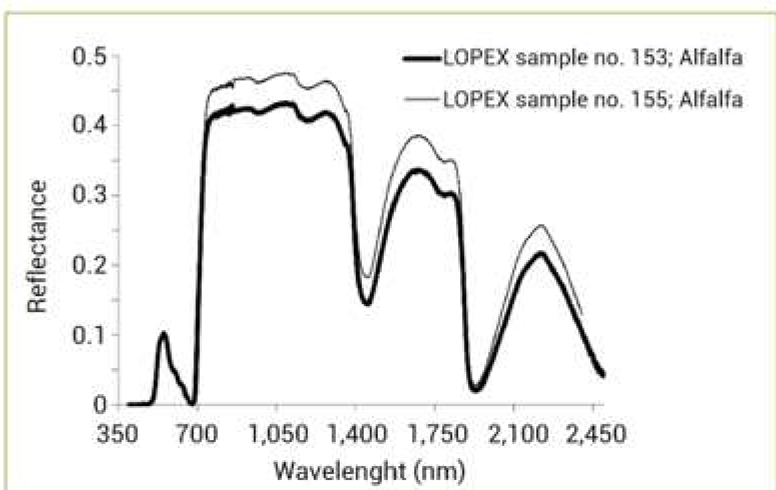

Figure 1. Samples of Alfalfa spectral reflectance curves.

Mobasheri, Mohammad Reza, and Sayyed Bagher Fatemi. 2013. 'Leaf Equivalent Water Thickness assessment using reflectance at optimum wavelengths', *Theoretical and Experimental Plant Physiology*, 25: 196-202.

Weighted average reflectance for NIR is 0.36

```
%%% estimate NIR reflectances for alfalfa

    midpt=[850, 1100,1300,1500,1700,1900,2050,2300];

    range =[300,200,200,200,200,200, 100,400];
```

```
midpt_m=midpt*10^-9;    % convert nanometers to meters

Emidpt=Planck(5700,midpt_m);

reflect=[0.4,0.4,0.4,0.2,0.35,0.3,0.05,0.2];

weight_ave3=sum(Emidpt.*reflect.*range)./sum(Emidpt.*range);
```

In lieu of direct measurements, we know NIR reflectance is a function of leaf N and alfalfa is an N fixer (Hollinger *et al.*, 2010). So we should adapt our value of leaf N to reflected NIR

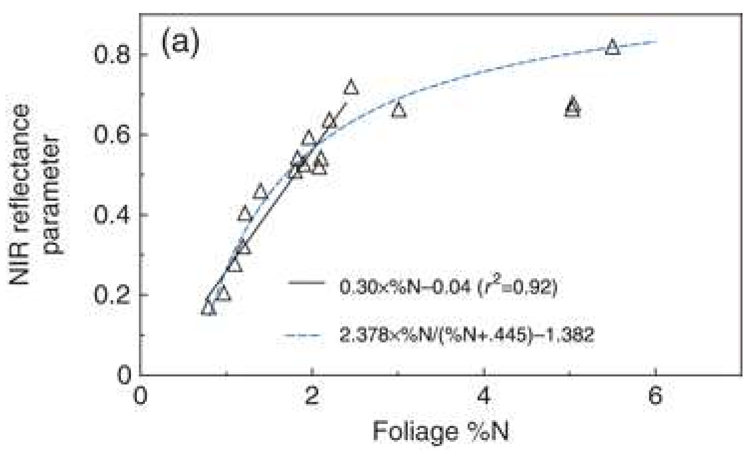

In producing model results we performed many tests on functions and variables to make sure we have the right units and they are functioning correctly

Histogram of NIR reflected by the canopy in the field

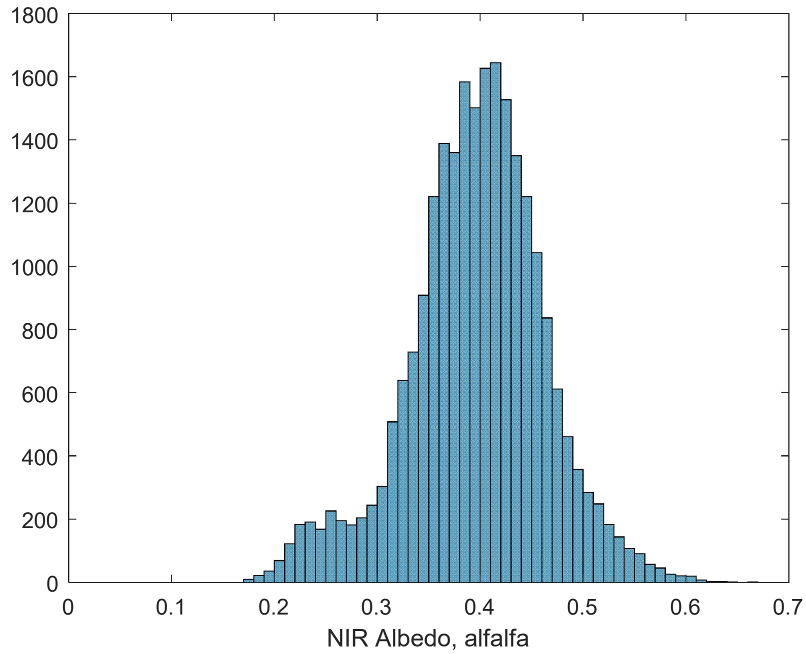

Doughty sees darkening of NIR in tropics with warming. What does change in NIR have on ET and Tsfc

Organic soil reflectance

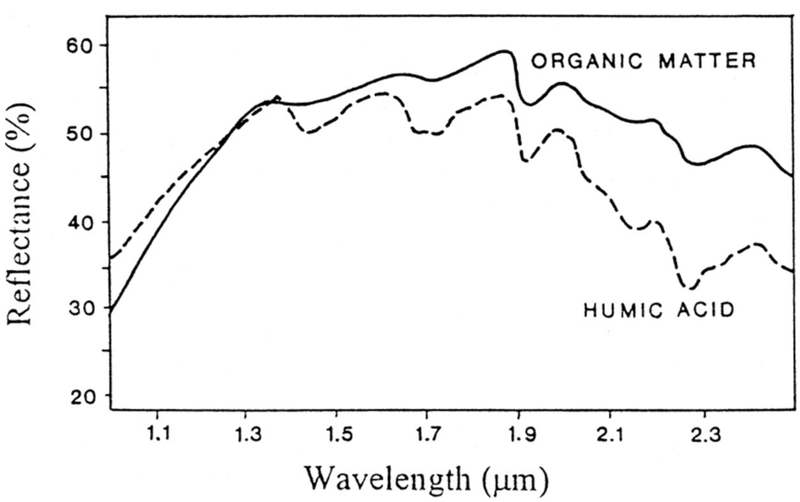

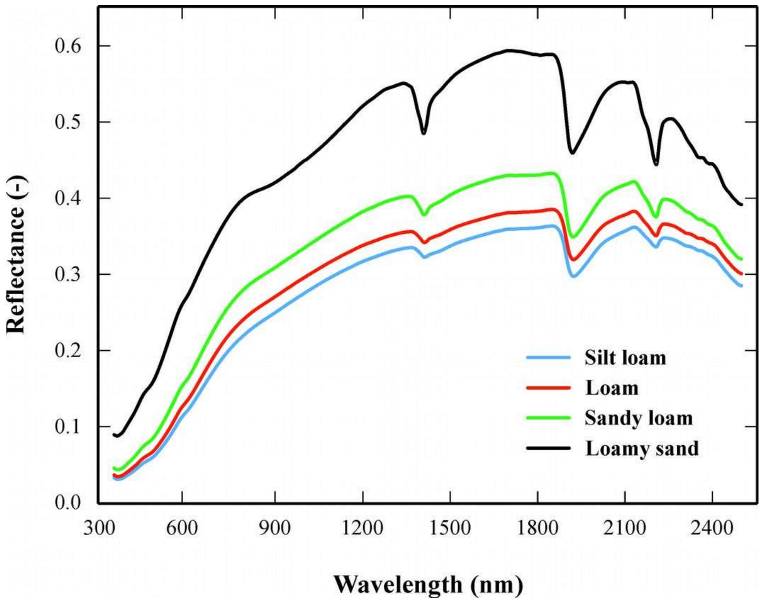

d2dest vs Tk

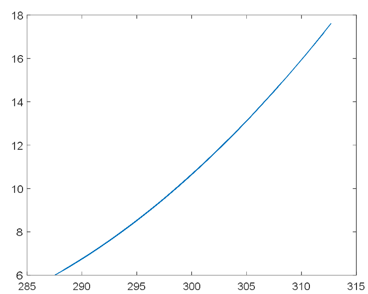

dest vs Tk, Pa/K

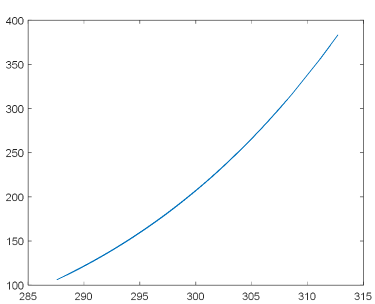

Leaf size was selected from papers in the literature as we did not have any direct measurements handy.

Typical leaf size

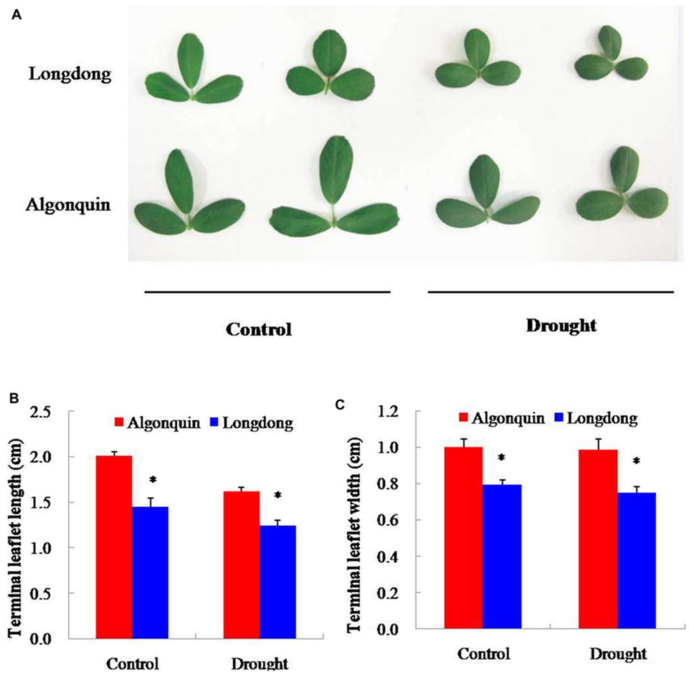

- DOI:10.3389/fpls.2015.01256

The dispersion matrix, Dij, was computed using a Lagrangian random walk model (Raupach, 1987, Raupach, 1989). This model requires we prescribe information on the heterogeneity of turbulent mixing in the canopy. Several authors have produced family portraits of these traits (Brunet, 2020, Finnigan, 2000, Raupach, 1988).

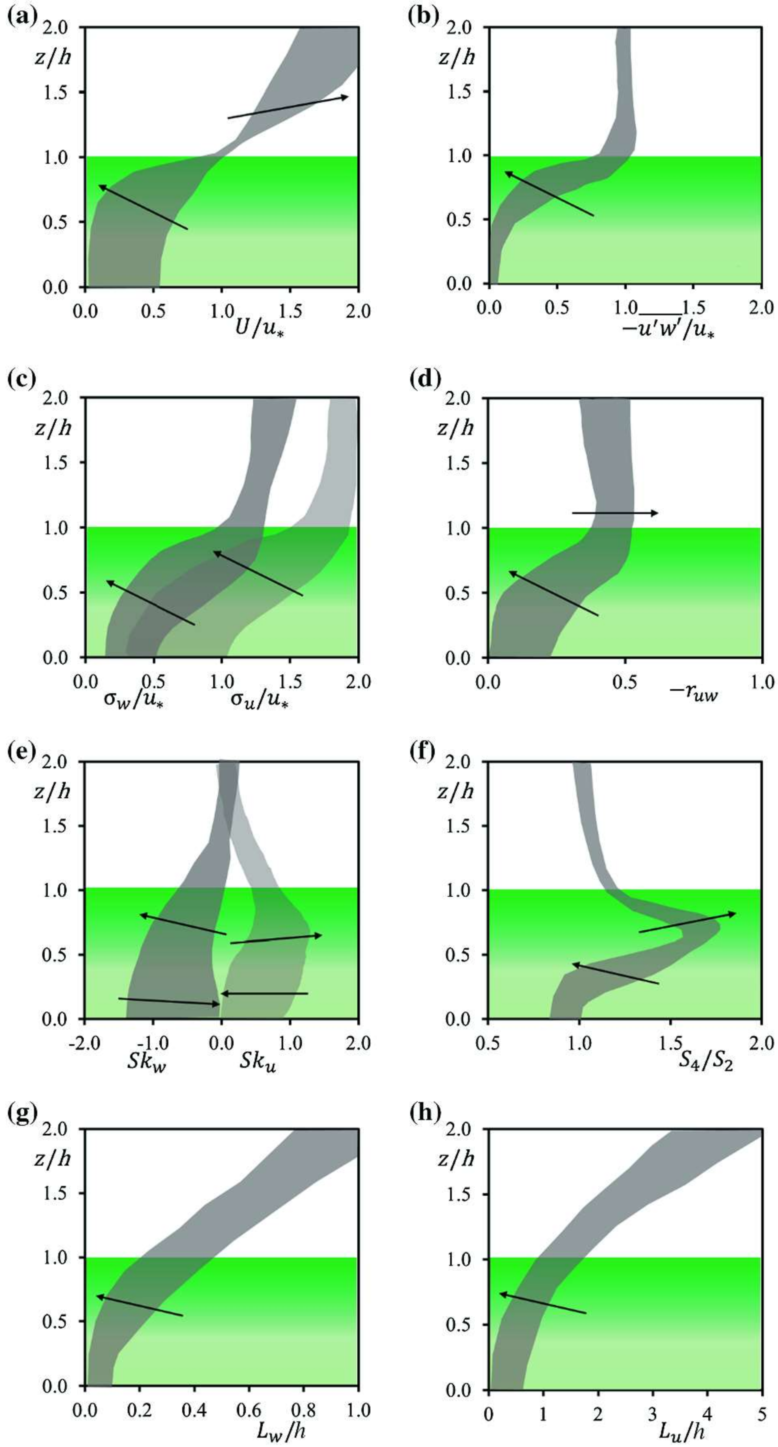

Because std w/u* is a function of stability, z/L, we ran the model for various stability conditions and produced a simple scaling function for the reference value, computed at u* equal 1 m/s and neutral conditions.

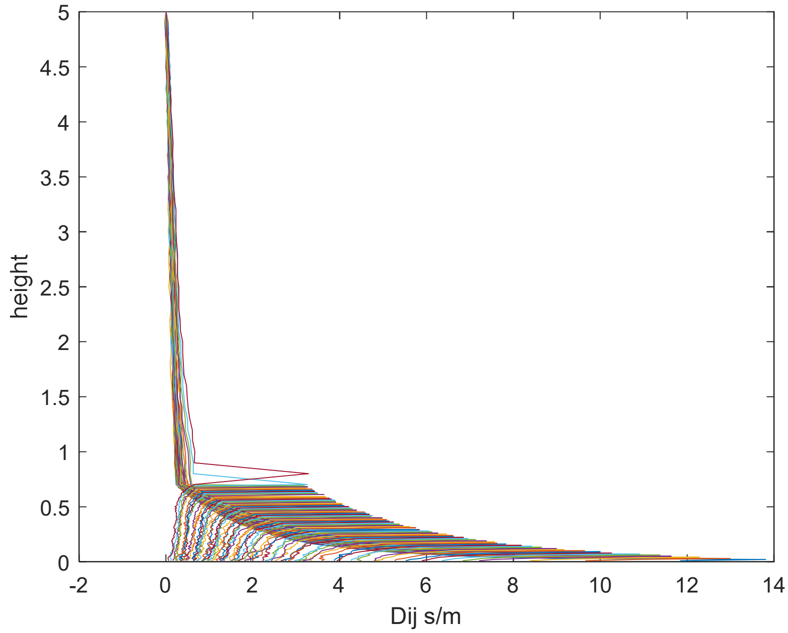

Because the height of the layers inside the canopy and atmosphere vary in this version with leaf area index, we need to recompute Dij for changes in leaf area index. Running 1,000,000 particles yields smoothest Dij

Dispersion Matrix, Alfalfa

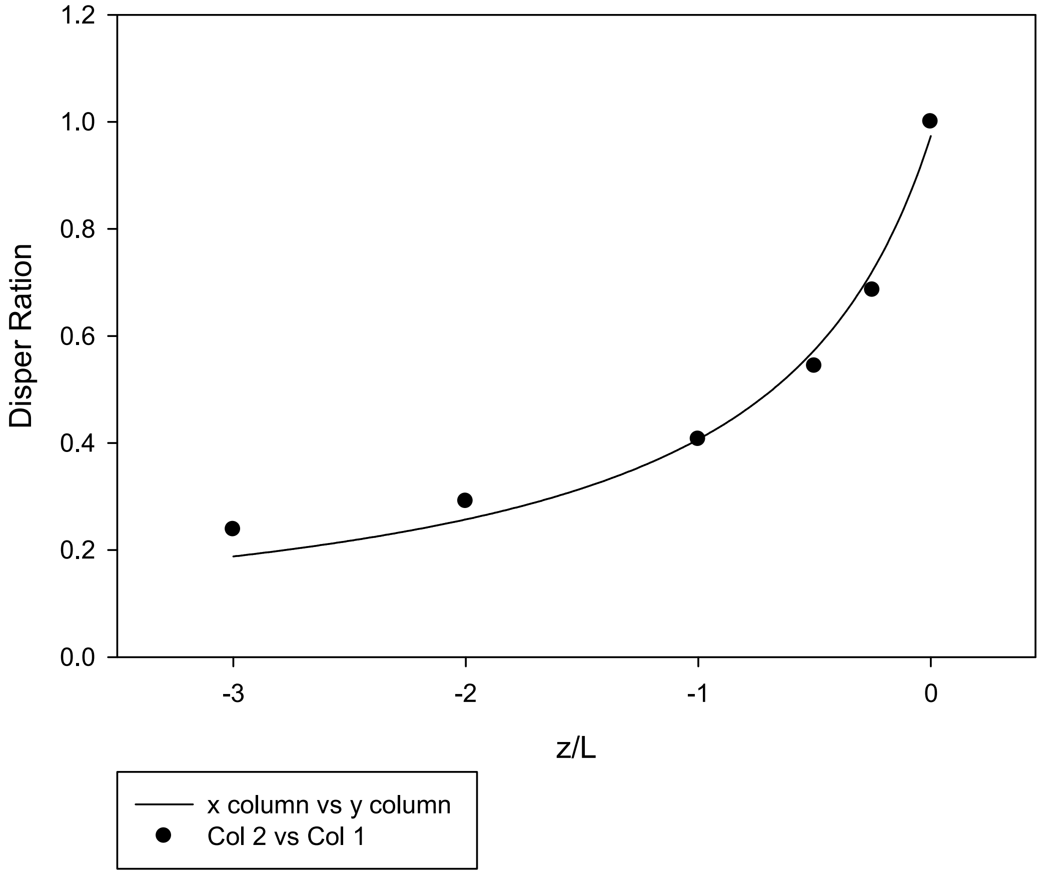

Nonlinear Regression

Data Source: Data 1 in Notebook1
Equation: Hyperbola, Hyperbolic Decay, 2 Parameter
f=(a*b)/(b+x)

R	Rsqr	Adj Rsqr	Standard Error of Estimate
0.9917	0.9836	0.9794	0.0407

	Coefficient	Std. Error	t	P	VIF
a	0.9735	0.0376	25.8669	<0.0001	1.8654
b	-0.7182	0.0881	-8.1523	0.0012	1.8654

Soil Heat Transfer

Adopting C code developed from Soil Physics in Basic (Campbell, 1985).

Also consulting new Python version of Campbell's work by Marco Bitelli

The complication I am having is matlab does not consider an index of zero in Arrays and the C and Python Code have that.

```
%%   fraction porosity + mineral + organic = 1

  %   airborne fraction = porosity - volumetric water content

        soil.bulkdensity=1.06;      % g cm-3   Data from Tyler Anthony
        soil.bulkdensity_kg_m3 = soil.bulkdensity *100*100*100/1000;

        soil.pore_fraction = 1-soil.bulkdensity/2.65;    %// from alfalfa, 1
minus ratio bulk density 1.00 g cm-3/2.65 g cm-3, density of solids


        soil.clay_fraction = .3;       %//  Clay fraction
        soil.peat_fraction = 0.08;     %//  SOM = a C; C = 4.7%, a = 1.72
Kuno Kasak, 2019 Bouldin Alfalfa


        soil.mineral_fraction= 1-soil.pore_fraction -soil.peat_fraction ; %
// from bulk density asssuming density of solids is 2.65


        soil.air_fraction = soil.pore_fraction - met.soilmoisture;

        soil.Cp_water= 4180;  % // J kg-1 K-1, heat capacity
        soil.Cp_air =  1065;
        soil.Cp_org = 1920;
        soil.Cp_mineral = 870;

        soil.K_mineral= 2.5;  % // W m-1 K-1, thermal conductivity
        soil.K_org= 0.8;
        soil.K_water= 0.25;
```

Corrected the parameter for computing the boundary layer resistance at the soil surface (Daamen & Simmonds, 1996). Our past work in Oregon found the need to apply this algorithm as soil get too hot without it. Heating causes convection that enhances heat transfer and acts as a feedback on surface temperature

```
%// Stability factor from Daamen and Simmonds 1996 WRR
% older parameterization was blowing up. Went back to original paper and
```

```
% coded it

        stabdel=5.*9.8*(prm.zht(1))*(soil.sfc_temperature-
soil.T_air)./((soil.T_air).*u_soil.*u_soil);
        %stabdel=0;


         epsilon(stabdel <=0) =-2 ;
         epsilon(stabdel > 0) =-0.75 ;

         epsilon=epsilon';
         z0_soil=0.001;

         Ram_soil=power(log(prm.zht(1)./z0_soil),2)./(0.4*0.4.*u_soil);

         Rh_soil=Ram_soil .* (1+stabdel).^epsilon;


        Rv_soil=Rh_soil;

        soil.Rv_soil=Rv_soil;
        soil.Rh_soil=Rh_soil;
```

Future work is to code up photosynthesis for corn, C4 (Collatz *et al.*, 1992, Yin & Struik, 2009, Zhou *et al.*, 2019)

Soil Info fro SoilWeb

https://casoilresource.lawr.ucdavis.edu/gmap/?loc=38.10034,-121.50163,z17

50% Ryde

Depth Range (cm)	Horizon Designation	Percent Clay	Percent Sand	Percent Organic Matter	pH by water Extraction	Sat. Hydraulic Conductivity (mm/hr)	EC (dS/m)	SAR (%)	Carbonates (% of < 2 mm)	Gypsum (% of < 20 mm)	CEC at pH 7 (cmol charge / kg soil)	K Factor	LEP	Oven-Dry D_b (g/cm^3)
0 - 20	*Ap*	*31*	*35*	*6*	*6.2*	*9.72*	*1*	*1*	*0*	*0*	*26.4*	*.20*	*3.1*	*1.44*
20 - 61	*A*	*31*	*35*	*6*	*6.2*	*9.72*	*1*	*1*	*0*	*0*	*26.4*	*.24*	*3.1*	*1.35*
61 - 81	*Ab*	*31*	*35*	*20*	*5*	*32.4*	*1*	*1*	*0*	*0*		*.24*	*2*	*0.68*

81 - 200	*Cg*	*33*	*15*	*20*	*7.2*	*32.4*	*1*	*1*	*0*	*0*	*41.9*	*.24*	*2.2*	*0.94*

[All Horizon Data]

35% Peltier

Depth Range (cm)	Horizon Designation	Percent Clay	Percent Sand	Percent Organic Matter	pH by water Extraction	Sat. Hydraulic Conductivity (mm/hr)	EC (dS/m)	SAR (%)	Carbonates (% of < 2 mm)	Gypsum (% of < 20 mm)	CEC at pH 7 (cmol charge / kg soil)	K Factor	LEP	Oven-Dry D_b (g/cm^3)
0 - 56	*Ap*	*31*	*35*	*17.5*	*6.5*	*32.4*	*1*	*1*	*0*	*0*	*46.4*	*.24*	*2.1*	*0.67*
56 - 61	*BA*	*40*	*8*	*16*	*6.7*	*3.276*	*1*	*1*	*0*	*0*	*48.4*	*.32*	*3.2*	*1.06*
61 - 114	*Bw*	*39*	*25*	*18*	*6.7*	*32.4*	*1*	*1*	*0*	*0*	*50.1*	*.20*	*3*	*0.76*
114 - 152	*2Cg*	*42*	*28*	*1*	*6.7*	*3.276*	*1*	*1*	*0*	*0*	*32.4*	*.28*	*6.7*	*1.7*

[All Horizon Data]

5% Rindge

We also have soil information from Kuno Kasak and Tyler Anthony

LAI of alfalfa.

B(1,2)

0.00153718160439161

11.7678244178294

```
LAI=0.001537*exp(11.76 * NDVIavg);
```

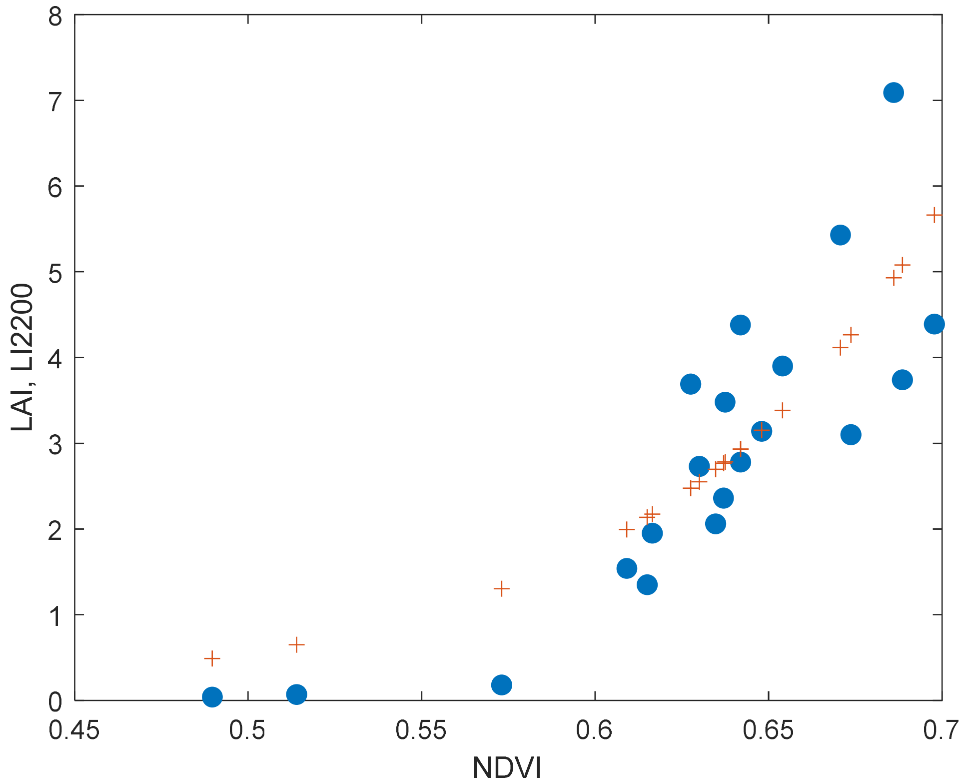

References

Baldocchi DD (1994) An analytical solution for coupled leaf photosynthesis and stomatal conductance models. Tree Physiology, **14**, 1069-1079.

Baldocchi DD, Bowling DR (2003) Modelling the discrimination of 13CO2 above and within a temperate broad-leaved forest canopy on hourly to seasonal time scales. Plant Cell and Environment, **26**, 231-244.

Baldocchi DD, Fuentes J, Bowling D, Turnipseed A, Monson R (1999) Scaling isoprene fluxes from leaves to canopies: test cases over a boreal aspen and a mixed temperate forest. Journal of Applied Meteorology, **38**, 885-898.

Baldocchi DD, Harley PC (1995) Scaling carbon dioxide and water vapor exchange from leaf to canopy in a deciduous forest: model testing and application. Plant, Cell and Environment, **8**, 1157-1173.

Baldocchi DD, Meyers T (1998) On using eco-physiological, micrometeorological and biogeochemical theory to evaluate carbon dioxide, water vapor and trace gas fluxes over vegetation: a perspective. Agricultural and Forest Meteorology, **90**, 1-25.

Baldocchi DD, Wilson KB (2001) Modeling CO2 and water vapor exchange of a temperate broadleaved forest across hourly to decadal time scales. Ecological Modeling, **142**, 155-184.

Baldocchi DD, Wilson KB, Gu L (2002) Influences of structural and functional complexity on carbon, water and energy fluxes of temperate broadleaved deciduous forest. Tree Physiology., **22**, 1065-1077.

Brunet Y (2020) Turbulent Flow in Plant Canopies: Historical Perspective and Overview. Boundary-Layer Meteorology, **177**, 315-364.

Campbell GS (1985) *Soil Physics with Basic,* Amsterdam, Elsevier.

Collatz GJ, Ball JT, Grivet C, Berry JA (1991) Physiological and environmental regulation of stomatal conductance, photosynthesis and transpiration: a model that includes a laminar boundary layer. Agricultural and Forest Meteorology, **54**, 107-136.

Collatz GJ, Ribas-Carbo M, Berry JA (1992) Coupled photosynthesis-stomatal conductance model for leaves of C4 plants. Australian Journal of Plant Physiology, **19**, 519-538.

Daamen CC, Simmonds LP (1996) Measurement of Evaporation from Bare Soil and its Estimation Using Surface Resistance. Water Resources Research, **32**, 1393-1402.

Farquhar GD, Caemmerer SV, Berry JA (1980) A Biochemical-Model of Photosynthetic Co2 Assimilation in Leaves of C-3 Species. Planta, **149**, 78-90.

Finnigan J (2000) Turbulence in Plant Canopies. Annu. Rev. Fluid Mech., **32**, 519-571.

Franks PJ, Bonan GB, Berry JA, Lombardozzi DL, Holbrook NM, Herold N, Oleson KW (2018) Comparing optimal and empirical stomatal conductance models for application in Earth system models. Global Change Biology, **0**.

Hollinger DY, Ollinger SV, Richardson AD *et al.* (2010) Albedo estimates for land surface models and support for a new paradigm based on foliage nitrogen concentration. Global Change Biology, **16**, 696-710.

Medlyn BE, Duursma RA, Eamus D *et al.* (2011) Reconciling the optimal and empirical approaches to modelling stomatal conductance. Global Change Biology, **17**, 2134-2144.

Norman JM (1979) Modeling the complete crop canopy. In: *Modification of the aerial environment of plants.* (ed B.J. Barfield and J.F. Gerber) pp Page. St. Joseph, MI, , American Society of Agricultural Engineering.

Norman JM (1981) Interfacing leaf and canopy light interception models. In: *Predicting Photosynthesis for Ecosystem Models.* (eds Hesketh JD, Jones JW) pp Page. Boca Raton, FL, CRC Press.

Norman JM (1993) Scaling processes between leaf and canopy. In: *Scaling physiological processes: leaf to globe.* (eds Ehleringer JR, Field C) pp Page., Academic Press.

Oikawa PY, Sturtevant C, Knox SH, Verfaillie J, Huang YW, Baldocchi DD (2017) Revisiting the partitioning of net ecosystem exchange of CO2 into photosynthesis and respiration with simultaneous flux measurements of (CO2)-C-13 and CO2, soil respiration and a biophysical model, CANVEG. Agricultural and Forest Meteorology, **234**, 149-163.

Paw U KT, Gao W (1988) Applications of solutions to non-linear energy budget equations. Agricultural and Forest Meteorology, **43**, 121-145.

Raschke K (1960) Heat Transfer Between the Plant and the Environment. Annual Review of Plant Physiology, **11**, 111-126.

Raupach MR (1987) A Lagrangian Analysis of Scalar Transfer in Vegetation Canopies. Quarterly Journal of the Royal Meteorological Society, **113**, 107-120.

Raupach MR (1988) Canopy transport processes. In: *Flow and Transport in the Natural Environment.* (eds Steffen W, Denmead OT) pp Page. Berlin, Springer-Verlag.

Raupach MR (1989) A Practical Lagrangian Method for Relating Scalar Concentrations to Source Distributions in Vegetation Canopies. Quarterly Journal of the Royal Meteorological Society, **115**, 609-632.

Sharkey TD, Bernacchi CJ, Farquhar GD, Singsaas EL (2007) Fitting photosynthetic carbon dioxide response curves for C(3) leaves. Plant, Cell & Environment, **30**, 1035-1040.

Xu L, Baldocchi DD (2003) Seasonal trend of photosynthetic parameters and stomatal conductance of blue oak (Quercus douglasii) under prolonged summer drought and high temperature. Tree Physiology*,* **23**, 865-877.

Yin X, Struik PC (2009) C3 and C4 photosynthesis models: An overview from the perspective of crop modelling. NJAS - Wageningen Journal of Life Sciences*,* **57**, 27-38.

Zhou H, Akçay E, Helliker BR (2019) Estimating C4 photosynthesis parameters by fitting intensive A/Ci curves. Photosynthesis research*,* **141**, 181-194.